

HOST-SYMBIONT CODIVERGENCE

A Novel Test for Host-Symbiont Codivergence Indicates Ancient Origin of Fungal Endophytes in Grasses

C. L. Schardl¹, K. D. Craven², S. Speakman³, A. Stromberg³,
A. Lindstrom³, and R. Yoshida³

¹*Department of Plant Pathology, 201F PSB, 1405 Veterans Drive,
University of Kentucky, Lexington, KY 40546-0312.*

²*Plant Biology Division, The Samuel Roberts Noble Foundation,
2510 Sam Noble Parkway, Ardmore, Oklahoma 73401.*

³*Department of Statistics, University of Kentucky, Lexington, KY 40526-0027*

CLS, KDC, SS and RY contributed equally to this work

Corresponding author: Ruriko Yoshida,

Department of Statistics, University of Kentucky, Lexington, KY 40526-0027

phone:(859) 257-5698, Fax:(859) 323-1973

email:ruriko@ms.uky.edu,

Abstract.— Significant phylogenetic codivergence between plant or animal hosts (H) and their symbionts or parasites (P) indicate the importance of their interactions on evolutionary time scales. However, valid and realistic methods to test for codivergence are not fully developed. One of the systems where possible codivergence has been of interest involves the large subfamily of temperate grasses (Pooideae) and their endophytic fungi (epichloae). These widespread symbioses often help protect host plants from herbivory and stresses, and affect species diversity and food web structures. Here we introduce the MRCALink (most-recent-common-ancestor link) method and use it to investigate the possibility of grass-epichloë codivergence. MRCALink applied to ultrametric H and P trees identifies all corresponding nodes for pairwise comparisons of MRCA ages. The result is compared to the space of random H and P tree pairs estimated by a Monte Carlo method. Compared to tree reconciliation the method is less dependent on tree topologies (which often can be misleading), and it crucially improves on phylogeny-independent methods such as **ParaFit** or the Mantel test by eliminating an extreme (but previously unrecognized) distortion of node-pair sampling. Analysis of 26 grass species-epichloë species symbioses did not reject random association of H and P MRCA ages. However, when five obvious host jumps were removed the analysis significantly rejected random association and supported grass-endophyte codivergence. Interestingly, early cladogenesis events in the Pooideae corresponded to early cladogenesis events in epichloae, suggesting concomitant origins of this grass subfamily and its remarkable group of symbionts. We also applied our method to the well-known gopher-louse data set.

key words: coevolution, grasses, endophytes, phylogenetic trees.

Symbioses between cool-season grasses (Poaceae subfamily Pooideae) and fungi of genus *Epichloë* (including their asexual derivatives in the genus *Neotyphodium*) are very widespread and occur in a broad taxonomic range of this important grass subfamily. These symbioses span the continuum from mutualistic to antagonistic interactions, making them an especially interesting model for evolution of mutualism, and particularly the possible role of codivergence (Jackson, 2004; Piano et al., 2005; Schardl et al., 1997; Sullivan and Faeth, 2004; Tredway et al., 1999). They have major ecological implications, affecting food web structures (Omacini et al., 2001) and species diversity (Clay and Holah, 1999). These endophytes extensively colonize host vegetative tissues without eliciting symptoms or defensive responses, and in many grass-epichloë symbiota the endophyte colonizes the embryos and is vertically transmitted with exceptional efficiency (Freeman, 1904; Sampson, 1933, 1937). The asexual endophytes rely upon vertical transmission for their propagation, whereas sexual (*Epichloë*) species are also capable of horizontal transmission via meiotically derived ascospores (Chung and Schardl, 1997). Mixed vertical and horizontal transmission strategies are also common. The tendency for vertical transmission is predicted to select for mutualism (Bull et al., 1991; Herre, 1993). In fact, many vertically transmitted, and even some horizontally transmitted epichloae help protect their hosts from herbivores, nematodes, and other stressors (Clay and Schardl, 2002). Grass-epichloë symbioses occur in most tribes of the Pooideae, the highly speciose subfamily of temperate C3 grasses. Most but not all *Epichloë* and *Neotyphodium* species are specialized to individual host species, genera or tribes in the Pooideae (Schardl and Leuchtman, 2005). Therefore, it is reasonable to hypothesize a history of Pooideae-epichloë coevolution extending back to the origin of this grass subfamily.

Previous analyses of the grass-epichloë system have suggested some codivergence, along with some host species transfers (jumps) (Jackson, 2004; Schardl et al., 1997). However, methods for such comparative phylogenetic studies are in need of refinement.

Interpreting evidence for codivergence based solely on congruence and reconciliation of tree topologies has significant shortcomings. Although tree reconciliation is useful particularly to assess strict cospeciation, precise mirror phylogenies for co-evolving hosts and symbionts can be an overly restrictive expectation (Legendre et al., 2002; Page and Charleston, 1998). For example, incomplete taxonomic sampling as well as lineage sorting of gene polymorphisms can result in topological incongruence between H and P trees, and deviations from strict cospeciation may mask tendencies for phylogenetic tracking. Refined methods are needed to assess significant patterns of codivergence without strict cospeciation. An attractive approach is to assess the correspondence in timing of cladogenesis events (Hafner et al., 1994). Methods that compare H and P pairwise distance matrices, e.g., by the Mantel test (Hafner et al., 1990) or ParaFit (Legendre et al., 2002), would seem to assess the timing of corresponding cladogenesis events directly. However, comprehensive pairwise distance methods suffer from grossly unequal sampling of corresponding cladogenesis events depending on the depth of the nodes representing those events in the actual H and P trees. The problem is illustrated by the simple examples in Figure 1 (and further documented in the Discussion). A statistical test for codivergence should evaluate the relationship between corresponding MRCA (most recent common ancestor) pairs without bias, but this is not equivalent to comparing matrices of all patristic distances between tree leaves (the extant sequences), simply because MRCAs deeper in the tree represent multiple descendant pairs, effectively weighting deeper (older) MRCAs over shallower MRCAs.

Here we introduce the MRCALink method to address the hypothesis that a group of hosts and symbionts (or parasites) have a significant degree of historical codivergence. The method is based on corresponding MRCA ages inferred from ultrametric maximum likelihood (ML) trees, but crucially samples each corresponding MRCA pair once and only once. From the set of sampled pairs of MRCA divergence

times in corresponding *H* and *P* trees, we estimate the probability of similarity between the H and P trees by using randomly generated trees from the tree space. We apply this method to the grass-epichloë system to assess evidence for codivergence and ancient origins of these symbioses. This same method is also applied to a well-known gopher-louse data set for comparison purposes.

METHODS

Fungal Endophyte Isolates and Endophyte-Infected Grasses

The cool-season grasses and their respective fungal endophytes are listed in Table 1. All endophytes examined were from natural infections from which the corresponding natural host plant, or leaf material from this plant was available for chloroplast sequence analysis. Representatives of all available *Epichloë* species and nonhybrid *Neotyphodium* species were included. In most cases where an *Epichloë* species infects multiple host genera, isolates from each genus were sampled. The sole exception was *E. typhina*, for which codivergence can be rejected a priori due to its broad host range (Leuchtman and Schardl, 1998; Craven et al., 2001). Many *Neotyphodium* species are interspecific hybrids, and therefore possess multiple genomes of distinct origin. These were usually excluded because of the difficulty in choosing the appropriate genome for analysis. However, four hybrid endophytes associated with *Lolium* species were included because they possess genomes in a clade (designated LAE, for *Lolium*-Associated Endophytes) that was unrepresented among those of known *Epichloë* species. Each of these four species – *Neotyphodium coenophialum*, *Neotyphodium occultans*, *Neotyphodium* sp. FaTG2 and *Neotyphodium* sp. FaTG3 – had a distinct history of interspecific hybridization (Tsai et al., 1994; Moon et al., 2000).

Sequencing of Chloroplast DNA (cpDNA) Non-Coding Regions

Genomic DNA was isolated from 0.5-1.0 g of harvested endophyte-infected plant leaf material by the CTAB method (Doyle and Doyle, 1990), and dissolved in 1 mL of

purified water (Milli-Q; Millipore Corp., Bedford, Massachusetts). DNA was quantified by bisbenzimidazole fluorescence, measured with a Hoefer (San Francisco, California) DyNA Quant 200 fluorometer.

PCR amplification of one intron (*trnL* intron) and two intergenic spacers (*trnT-trnL*, *trnL-trnF*) from cpDNA was performed from total plant DNA with primers described by Taberlet et al. (1991). Reactions were performed in 50 μ L volumes containing 15 mM Tris-HCl, 1.5 mM MgCl₂, 50 mM KCl, pH 8.0 in the presence of 200 μ M of each dNTP (Panvera, Madison, Wisconsin), 200 nM of each primer (Integrated DNA Technologies, Coralville, Iowa), 1.25 unit Amplitaq Gold DNA polymerase (Applied Biosystems, Foster City, California), and 10 ng of genomic DNA. Reactions were performed in a PE Applied Biosystems DNA thermal cycler, with a 9 min preheat step at 95°C to activate the enzyme, followed by 35 cycles of 1 min at 95°C, 1 min at 55°C, and 1 min at 72°C. All amplification products were verified by 0.8% agarose gel electrophoresis, followed by visualization with ethidium bromide staining and UV fluorescence. The concentration of amplified products was estimated by comparison with a 100 bp quantitative ladder (Panvera). The amplified cpDNA products were purified with Qiaquick spin columns (Qiagen Inc., Valencia, California), then sequenced by the Sanger method with a BigDye Terminator Cycle version 1.0 or 3.1 sequencing kit (Applied Biosystems) or CEQ 2000 Dye Terminator Cycle Sequencing kit (Beckman-Coulter, Fullerton, California). The primers used in PCR were also used in sequencing, along with several primers designed for internal sequencing of amplified cpDNA fragments (Table 2). Both DNA strands were sequenced. Products were separated by capillary electrophoresis on an Applied Biosystems model 310 genetic analyzer or on a CEQ 8000 genetic analyzer (Beckman-Coulter) at the University of Kentucky Advanced Genetic Technologies Center. Sequences were assembled with either Sequence Navigator software (Applied Biosystems) or Phrap (CodonCode Corporation, Dedham, Massachusetts). Sequences were entered into GenBank as accession numbers

AY450932–AY450949 and EU119353–EU119377.

Endophyte DNA Sequences

β -Tubulin and translation-elongation factor 1- α gene sequences for the endophytes included in this study were obtained previously (Craven et al., 2001; Moon et al., 2004). Employing a standardized gene nomenclature for *Epichloë* and *Neotyphodium* species, these genes are designated *tubB* (formerly *tub2*) and *tefA* (formerly *tef1*), respectively.

Phylogenetic Tree Reconstruction and Analysis

Sequences were aligned with the aid of PILEUP implemented in SEQWeb Version 1.1 with Wisconsin Package Version 10 (Genetics Computer Group, Madison, Wisconsin). PILEUP parameters were adjusted empirically; a gap penalty of two and a gap extension penalty of zero resulted in reasonable alignment of intron-exon junctions and intron regions of endophyte sequences, and of intergenic spacer and intron regions of cpDNA sequences. Alignments were scrutinized and adjusted by eye, using tRNA or protein coding regions as anchor points. For phylogenetic analysis of the symbionts, sequences from *tubB* and *tefA* were concatenated to create a single, contiguous sequence of approximately 1400 bp for each endophyte, of which 357 bp was exon sequence and the remainder was intron sequence. For phylogenetic analysis of the hosts, sequences for both cpDNA intergenic regions (*trnT-trnL* and *trnL-trnF*) and the *trnL* intron were aligned individually then concatenated to give a combined alignment of approximately 2200 bp.

Ultrametric trees were inferred with BEAST v1.4.1 (Drummond and Rambaut, 2007) with the general time reversible model with a proportion of invariable sites and a gamma distributed rate variation among sites (GTR+I+G). This model was selected by the software MrModelTest vers. 2.0 (Johan A. A. Nylander, Uppsala University, <http://www.csit.fsu.edu/nylander/mrmodeltest2readme.html>)(Posada and Crandall,

1998) as the model of nucleotide substitution that best fits the data. Based on published phylogenetic inference for the grass subfamily Pooideae (Soreng and Davis, 1998), *Brachyelytrum erectum* was chosen as the outgroup for the grass phylogenies. The corresponding endophyte, *Epichloë brachyelytri*, was the outgroup chosen for endophyte phylogenies. Due to the lack of historical dates for interior nodes, **BEAST** used a fixed substitution rate to reconstruct the trees. This results in branch lengths (and tree height) being measured in substitutions per site. The Markov chain Monte-Carlo method used by **BEAST** was allowed to run for 5,000,000 steps. Every 1000th step was recorded and analyzed for height, tree likelihood, and many other components. Preceding these recordings is a burn-in period equal to 10% of the MCMC chain. All data from the burn-in period are discarded and the operators are not optimized during this time, thus preventing operators from optimizing incorrectly on trees that are still considered random at the beginning of each run. This process was done two independent runs from different tree topologies in order to avoid stacking at a local optimum, and resulted in a sample of 10,000 trees.

The MRCALink algorithm reported herein requires ultrametric trees. However, for illustrative purposes only, phylograms were also inferred and posterior probabilities estimation with MrBayes version 3 (Ronquist and Huelsenbeck, 2003), using a GTR+G model (lset nst = 6, rates = gamma). Four chains (three heated at temp = 0.2) were run for 450,000 generations, saving one out of every 100 trees (mcmc ngen = 450,000, printfreq = 10,000, samplefreq = 100, nchains = 4). The first 2000 trees (200,000 generations) were discarded as burn-in. This was an extremely conservative choice because likelihood values stabilized within 10,000 generations for both datasets. The 50% majority rule consensus trees and posterior support values were determined from the 2500 trees sampled from the remaining 250,000 generations. We ran each three independent runs with 200,000 iterations and always got the same consensus tree as shown in Figure 2 and 3.

Sequence alignments and trees reconstructed via **MrBayes** and **BEAST** of plants and endophytes have been submitted to TreeBASE.

The MRCALink Algorithm

The MRCALink algorithm introduced here identifies and stores each corresponding H and P MRCA pair. Crucially, the data for each corresponding MRCA pair are selected only once for subsequent statistical analysis. For example, if we have pairs of trees in Figure 1, then we pick MRCA pair $(7, 7')$ in the congruent tree four times from the set of all pairs of taxa in H and P . The MRCALink algorithm picks $(7, 7')$ only once instead of four times. Ultrametric H and P trees must be used so that a unique age is estimated for each MRCA as half the patristic distance between any two of its descendant leaves. Trees must be strictly bifurcating for unique identification of valid H and P MRCA pairs. The **BEAST** program outputs ultrametric and strictly bifurcating trees. Note that the method does not assume an equal number of taxa in H and taxa in P , and also does not assume similar substitution rates in H and P . Please see Appendix for the pseudo-code of the algorithm.

Source codes for The MRCALink algorithm and the dissimilarity methods as well as data files are available at <http://www.ms.uky.edu/~ruriko/MRCALink/>.

Significance of Codivergence

In this section we will discuss the two statistical methods used to test significance of codivergence between the host and the parasite sets. The first is a dissimilarity estimate between trees in the same treespace. The second test uses **ParaFit** (Legendre et al., 2002) to analyze the MRCA pairs sampled by the MRCALink algorithm. The hypotheses are:

Null hypothesis: Trees T_H and T_P are independent.

Alternative hypothesis: Trees T_H and T_P are not independent.

Test via the dissimilarity method.— We are interested in estimating the probability that the host and symbiont tree have some degree of dependence that may be due to a history of codivergence. To this end, we use the sets of all pairwise differences in H and P or the sets of pairwise differences in H and P from the MRCA pairs sampled by the MRCALink algorithm. Let the sum of differences in uniquely estimated MRCA ages for trees A and B be $S(A, B)$. The null hypothesis is that our T_H and T_P are independent, so we generate a distribution of S for pairs of unrelated random trees with the same number of leaves and root-to-tip normalized distances (i.e., we normalize the heights of T_H and T_P to 1) as T_H and T_P . Then we compare our $S(T_H, T_P)$ with this distribution. If the p-value is significantly low (< 0.05), we reject the null hypothesis and conclude that there is evidence of codivergence between T_H and T_P . To calculate $S(A, B)$ with all pairwise distances, we take the sum of differences between pairwise distances for A and B over all pairwise distances. To calculate $S(A, B)$ with the set of the MRCA pairs sampled by the MRCALink algorithm we take the sum of differences between pairwise distances for A and B over the set of the MRCA pairs sampled by the MRCALink algorithm.

We generate 10,000 random trees with the given branch lengths from the birth and death process (BDP) via **evolver** from the PAML package (Yang, 1997) for each T_H and T_P . For each tree, we used birth rate 0.5, death rate 0.5, and sampling fraction (SF = ratio of sample size to population size) 1, 0.5, 0.001, or 0.0005. We use the BDP model because it is biologically plausible (Aris-Brosou and Yang, 2003; Yang and Rannala, 1997) (also see more details on the Discussion section).

Note the CPU time of this estimation with all pairwise distances is $O(Rn^2)$ and with the MRCALink algorithm it is $O(Rn^4)$, where R is the number of random trees and n is the largest number of taxa in H or P (i.e., $n = \max\{n_1, n_2\}$ where n_1 is the number of taxa in H and n_2 is the number of taxa in P). The CPU time of the dissimilarity method is a polynomial time algorithm in terms of the number of taxa.

Also note that this process is easily distributed. Thus, if we fix R the computation time of this method with all pairwise distances is $O(n^2)$ and the method with the MRCALink algorithm is $O(Rn^4)$.

Testing via ParaFit.— The **ParaFit** (Legendre et al., 2002) method requires three input files: a relation table designating the hosts and their parasites, and the coordinate representation of phylogenetic distances for H and P . These are the results of PCA (Principle Component Analysis) on the respective distance matrices. This method has been applied with all $\binom{n_1}{2}$ pairwise distances between two taxa in H and all $\binom{n_2}{2}$ pairwise distances between two taxa in P . Instead, we use the distance matrices for H and P computed from the set of MRCA pairs via the MRCALink algorithm.

The following is an example of a distance matrix for all pairwise distances between any two taxa of a tree with 4 taxa. d_{ij} represents a pairwise distance between taxa i and j .

$$\begin{pmatrix} 0 & d_{12} & d_{13} & d_{14} \\ d_{12} & 0 & d_{23} & d_{24} \\ d_{13} & d_{23} & 0 & d_{34} \\ d_{14} & d_{24} & d_{34} & 0 \end{pmatrix}$$

Below is the same distance matrix using only the set of MRCA pairs provided by the MRCALink algorithm as used on the congruent tree in Figure 1. Notice the removal of the distances between the sets of taxa (1,4), (2,3), and (2,4). These represent the redundant information removed by the MRCALink algorithm. The sets of taxa (1,3), (1,4), (2,3), and (2,4) all have the same MRCA. The distance between taxa 1 and 3 is sufficient and is the only one used in this reduced distance matrix.

$$\begin{pmatrix} 0 & d_{12} & d_{13} & \mathbf{0} \\ d_{12} & 0 & \mathbf{0} & \mathbf{0} \\ d_{13} & \mathbf{0} & 0 & d_{34} \\ \mathbf{0} & \mathbf{0} & d_{34} & 0 \end{pmatrix}$$

Following is another distance matrix using only the set of MRCA pairs provided by the MRCALink algorithm as used on the incongruent tree in Figure 1. Notice the removal of the distances between the sets of taxa (2,3) and (2,4). These represent the redundant information removed by the MRCALink algorithm. The MRCALink algorithm has a smaller effect on less congruent trees.

$$\begin{pmatrix} 0 & d_{12} & d_{13} & d_{14} \\ d_{12} & 0 & \mathbf{0} & \mathbf{0} \\ d_{13} & \mathbf{0} & 0 & d_{34} \\ d_{14} & \mathbf{0} & d_{34} & 0 \end{pmatrix}$$

Random Tree generators for the CPU time test

We generated random trees with 200 taxa by BDP with 0.5 birth rate, 0.5 death rate, and 0.0001 sampling fraction because Aris-Brosou and Yang (2003), and Yang and Rannala (1997) suggested that this is realistic model to generate random phylogenetic trees. The heights of the trees are the same as T_H and T_P in the T_4 data set. Since the computational time was 4-7 hours, we only took two sets of random trees for T_H and T_P and then we recorded the CPU time.

RESULTS

Grass Phylogenies

PCR amplification of *trnT-trnL* and *trnL-trnF* intergenic spacers and the *trnL* intron from endophyte-infected host plant genomic DNA yielded products of the sizes expected (approximately 850-950 bp, 400-450 bp for *trnT-trnL* and *trnL-trnF*, respectively; 350-600 bp for the *trnL* intron). The majority rule consensus tree with average branch lengths from MrBayes search on host cpDNA sequences is shown in Figure 2. In general, the inferred relationships among grass tribes were in good

agreement with published grass phylogenies inferred by various genetic criteria (Soreng and Davis, 1998; Kellogg, 2001; Catalán et al., 2004). Host grasses in the tribes Poeae, Agrostideae (syn = Aveneae), and Bromeae all formed monophyletic clades. Two of the three grasses in tribe Hordeae (syn = Triticeae) – *Hordeum brevisubulatum* and *Elymus canadensis* – also grouped in a well-supported clade. However, *Hordelymus europaeus*, currently classified in the Hordeae, grouped in the Bromeae clade basal to the *Bromus* species.

Among the grasses in the tribe Poeae, a clear phylogenetic separation between the fine-leaf fescues (*Festuca* subg. *Festuca*) and the broad-leaf fescues (*Lolium* subg. *Schedonorus* = genus *Schedonorus*) was evident (Figure 2). Among the broad-leaf fescues in this analysis were three hexaploids previously classified as *Festuca arundinacea*, and representing plants from Europe (shown as *L. arundinaceum*), southern Spain (*Lolium* sp. P4074) and Algeria (*Lolium* sp. P4078) (Tsai et al., 1994). The latter two plants had closely related cpDNA sequences in a subclade basal to the European plant and species of *Lolium* subg. *Lolium*. Given this relationship, plants P4074 and P4078 are listed here as an undescribed *Lolium* species. The Poeae clade also had *Holcus mollis* in a basal position, which was the sister to the Agrostideae clade.

The precise branching order of the most deeply rooted grasses was poorly resolved (Figure 2). The exception was *Brachypodium sylvaticum* (tribe Brachypodieae), which was placed nearest the clade comprising tribes Agrostideae, Poeae, Hordeae and Bromeae. This result agreed with published studies (Soreng and Davis, 1998; Kellogg, 2001), which also indicate that tribe Brachyelytreae (represented by *Be. erectum*) diverged very early in the evolution of the cool-season grasses. Therefore, we chose *Be. erectum* to outgroup root the grass phylogeny.

Endophyte Phylogenies

The combined sequence data set (*tubB* + *tefA*) for the epichloae was

approximately 1400 bp in length. The majority rule consensus tree from MrBayes search on the combined sequences (Figure 3) was in accord with the individual gene trees published earlier (Moon et al., 2004). Two large clades of the epichloae were well supported, and included only isolates from corresponding clades of the grasses. One of these included several species associated with either Agrostideae or its sister tribe Poeae, or both. This clade included *E. baconii*, *E. amarillans*, *E. festucae* and its closely related asexual species *N. lolii*, as well as an *Epichloë* sp. isolate from *Holcus mollis*. Also included in this clade was the LAE (*Lolium*-associated endophyte) subclade of sequences from asexual symbionts of *Lolium* species. The endophytes with LAE genomes were all interspecific hybrids with additional genomes from *E. festucae*, *E. typhina* or *E. bromicola*; species that have contributed genomes to a large number of hybrid endophytes (Moon et al., 2004). Because the LAE genomes have not been identified in any sexual (*Epichloë*) species, it is possible that the clade represents an old asexual lineage. If so, the LAE genome is very likely to have been transmitted vertically, because asexual epichloae are only known to transmit vertically in host maternal lineages (Chung and Schardl, 1997; Brem et al., 1999).

Another clade grouped endophytes from sister grass tribes Bromeae and Hordeae. This clade included *E. elymi*, *E. bromicola*, and asexual endophytes from *Bromus purgans*, *He. europaeus*, and *H. brevisubulatum*.

Epichloë glyceriae and *Neotyphodium gansuense*, infecting grasses in tribes Meliceae and Stipeae respectively, were placed at basal positions relative to the other endophyte species. Another basal clade grouped *E. typhina* from *L. perenne* with *E. sylvatica* and two asexual endophytes, *Neotyphodium typhinum* and *Neotyphodium aotearoae*.

Comparison of Endophyte and Host Tree Topologies

Several major groups or clades in the endophyte phylogeny corresponded to clades within the host phylogeny (Figure 4). For example, sister host tribes Agrostideae

and Poeae mostly coincided with a similar grouping of their endophytes. Within tribe Poeae, a group containing *L. multiflorum*, *L. arundinaceum*, and *Lolium* sp. plants P4074 and P4078 was mirrored by the branching orders of their respective LAE-clade endophytes. The sister clade relationship of *Lolium* and *Festuca* species was reflected by the LAE and *E. festucae* sister clades, and the basal position of *Hol. mollis* within tribe Poeae was nearly matched by that of its corresponding symbiont. Similarly, endophytes of the sister tribes Bromeae and Hordeae grouped in a clade. Grasses in basal host tribes Brachyelytreae, Stipeae, and Meliceae corresponded to basal endophyte clades *E. brachyelytri*, *N. gansuense*, and *E. glyceriae*, respectively.

Several instances of incongruence between host and endophyte phylogenies were also evident both within and across clades (Figure 4). Notable cases involved *E. typhina* and two related asexual endophytes, *N. typhinum* and *N. aotearoae*. All three of these endophytes infect grasses in tribes Poeae (*E. typhina* and *N. typhinum*) or Agrostideae (*N. aotearoae*), yet they grouped in a clade that was maximally divergent from the larger clade of endophytes from these grass tribes. Other examples of incongruence involved an *E. festucae* isolate from *Koeleria cristata* (tribe Agrostideae), *N. lolii* (an asexual derivative of *E. festucae*) from *L. perenne*, and *E. elymi* from *Bro. purgans*.

Analyses of Codivergence

Computation results.— For each data set, we generated 10,000 ultrametric trees through BEAST and chose the tree that had the maximum likelihood (Figure 4). From this tree, we obtained corresponding pairs of *H* (grasses) and *P* (endophytes) MRCA ages (plotted in Figure 5). The significance of codivergence was estimated from randomly generated tree pairs with several sampling fractions (Table 3). The lowest sampling fraction is probably the most biologically relevant (Aris-Brosou and Yang, 2003). We denote SF as a sampling fraction. We first estimated p-values via the dissimilarity methods. For the full grass and endophyte trees at SF = 0.0005, we estimated $p = 0.123$ with the MRCALink algorithm and $p = 0.784$ with all pairwise

distances. Thus, analysis of this data set did not reject the null hypothesis that the host and the parasite trees are independent.

An obvious source of discordance between endophyte and host trees was *E. typhina* and related endophytes. Both *N. lolii* and the *E. typhina* isolate in this study were from *L. perenne*, but the endophytes were maximally divergent from one another. Previous surveys have indicated that *E. typhina* has an unusually broad host range, and is ancestral to asexual endophytes (such as *N. typhinum*) in several other grasses (Leuchtman and Schardl 1998; Moon et al. 2004; Gentile et al. 2005). Therefore, the first trimmed tree set, T_1 , had these taxa removed, and the host and endophyte T_1 trees were estimated. Analysis of the T_1 set gave lower p-values ($p < 0.001$ with the MRCALink algorithm and $p = 0.117$ with all pairwise distances) (Table 3). Thus, the MRCALink analysis of this dataset supported dependence of the trees, although analysis with all pairwise distances did not. The hypothesis that the entire clade including *E. typhina*, *N. typhinum*, *E. sylvatica*, and *N. aotearoae* contributed most of the discordance was tested by eliminating all four of these taxa and their hosts in tree set T_2 . The calculated p-values for T_2 ($p < 0.001$ with MRCALink and $p = 0.093$ with all pairwise distances) were comparable to those of T_1 .

Trimmed set T_3 had *E. typhina* and *N. typhinum* and their hosts removed, as well as other taxa that appeared likely to represent jumps of endophytes between divergent hosts; namely *N. lolii* and its host *L. perenne*, the *E. festucae*-*K. cristata* symbiotum, and the *E. elymi*-*Bro. purgans* symbiotum. The basis for considering these to be likely jumps was that the symbiont species were much more common on other grass genera: *E. festucae* on *Festuca* species, and *E. elymi* on *Elymus* species (Craven et al., 2001; Moon et al., 2004). The p-values for the taxa in the T_3 set were $p < 0.001$ (Table 3) with the MRCALink algorithm and $p = 0.064$ with all pairwise distances (Table 3). Removal of all taxa that had been removed for T_2 and T_3 gave set T_4 , for which we found significant evidence to reject the null hypothesis by both approaches.

If codivergence has been an important trend since the origin of the epichloae and the pooid grasses, and if the DNA regions analyzed for these fungi and their hosts have had comparable substitution rates in the regions analyzed, then the estimated heights (h) of their respective phylogenetic trees should be comparable. Very different tree heights could be due to a lack of long-term codivergence of H and P , or to a large difference in substitution rates for the regions chosen for analysis. The tree heights estimated by BEAST in substitutions per site were as follows: for the full data set, $h(T_H) = 0.048623$ and $h(T_P) = 0.028991$; for T_1 , $h(T_H) = 0.046534$ and $h(T_P) = 0.028633$; for T_2 , $h(T_H) = 0.045813$ and $h(T_P) = 0.028924$; for T_3 , $h(T_H) = 0.048321$ and $h(T_P) = 0.028367$; for T_4 , $h(T_H) = 0.045188$ and $h(T_P) = 0.027939$. Thus, for all of these data sets the inferred host tree heights were similar, and the inferred endophyte tree heights were similar. For both hosts and endophytes, almost all of the sequence analyzed was noncoding. The host data set was mainly intergenic sequence from chloroplast DNA, and most of the endophyte data comprised nuclear intronic sequence. The tree height estimates suggested that the substitution rate of the host sequences has been 1.58 to 1.70 times the substitution rate of the endophyte sequences. Thus, the estimated substitution rates were comparable, lending additional support to the hypothesis that the Pooideae and the epichloae originated at approximately the same time.

We tested if the analyses reject sub-optimal parasite and host trees with no detectable host jumps. Instead of choosing the tree with maximum likelihood, we chose the three samples with likelihood values closest to the mean of likelihood values from the set of all trees sampled by BEAST. For example, the maximum likelihood tree for the full plant data set that was used in our methods had a negative log likelihood of -6771.2947. The sub-optimal samples had negative log likelihoods of -6783.4135, -6783.4134, and -6783.4076. We then calculated p-values by the dissimilarity method (Table 4) and ParaFit (Table 5).

Application of the dissimilarity methods to the sub-optimal trees did not provide

evidence to reject the null hypothesis (Table 4). The dissimilarity method with the MRCALink algorithm obtained significant p-values for some but not all samples. Computations were conducted on a Dual Core Pentium L2400 1.66 GHz PC machine in IBM Thinkpad laptop X60S with 2 GB RAM running Fedora Core 6 Linux. For the dissimilarity method with all pairwise distances, calculating the p-value has the time complexity $O(n^2)$ where n is the largest number of taxa in H or P (i.e., $n = \max\{|H|, |P|\}$). Thus, this is a polynomial time algorithm in terms of the number of taxa. Analyses of grass-endophyte data sets with the dissimilarity method with all pairwise distances required CPU time of 39.5 sec for the full 26 taxon pairs, 33.481 sec for T_1 , 27.2 sec for T_2 , 25.0 sec for T_3 , and 20.1 sec for T_4 . For computational time simulation analysis of our method with randomly generated 200-taxon trees with all pairwise distances, the dissimilarity method took 3.59 hr of CPU time.

For the dissimilarity method with the MRCALink algorithm, calculating the p-value has the time complexity $O(n^4)$ where n is the largest number of taxa in H or P (i.e., $n = \max\{|H|, |P|\}$). Thus, this is also a polynomial time algorithm in terms of the number of taxa. Analyses of grass-endophyte data sets with the MRCALink algorithm required CPU time of 2 min 49 sec for the full 26 taxon pairs, 2 min 16 sec for T_1 , 1 min 41 sec for T_2 , 1 min 33 sec for T_3 , and 1 min 9 sec for T_4 . The CPU time of our method with 200 taxa was 7 hr.

Note that to estimate the p-value using random trees, we can easily distribute computations for both methods. Thus, this estimation method could be applied to host-parasite associations with several hundred taxa.

Results with ParaFit.— We also analyzed the full grass and endophyte data sets T_1 through T_4 with **ParaFit**, again using either all pairwise patristic distances or only those selected by MRCALink. For the former, we used **ParaFit** with distance matrices for the data sets H and P after applying the PCA to their distance matrices. For the latter, we substituted 0 for some elements in order to represent only the set of MRCA

pairs sampled by the MRCALink algorithm. Note that **ParaFit** takes the PCA, not distance matrices, so even if we remove some elements the resulting PCA differs. Both approaches gave p-values all < 0.001 , indicating rejection of the null hypothesis. Thus, **ParaFit** appeared to be highly sensitive to any dependence between trees.

Most p-values for the sampled sub-optimal trees were significantly higher than p-values for the ML trees. The p-value of sample 1 from the T_4 data set was especially high compared to the p-value with the respective ML trees (Table 5).

Results with Gopher-Louse Data Sets

We also tested our methods with a well-known gopher-louse data set. The data set in Hafner et al. (1994) (full data set) contains 17 taxa of lice and 15 taxa of gophers, whereas Huelsenbeck et al. (2003) have trimmed host-parasite pairs representing apparent host jumps: louse species *Geomydoecus thomomys*, *Geomydoecus actuosi*, *Thomomydoecus barbarae* and *Thomomydoecus minor*, and gopher species *Thomomys talpoides* and *Thomomys bottae*.

To reconstruct trees, we used **BEAST** with the GTR+I+G model (Figure 6). In this analysis, *T. talpoides* and *T. bottae* were outgroups in the gopher data set, and *T. barbarae* and *T. minor* were outgroups in the louse data set. With the full data sets, application of **ParaFit** to all pairwise distances gave $p = 0.001$. In contrast, the dissimilarity method with the sampling fraction 0.0005 gave $p = 0.589$, not rejecting the null hypothesis (Table 6). With the trimmed data sets, application of **ParaFit** to all pairwise distances gave $p = 0.001$ and also the dissimilarity method with the sampling fraction = 0.0005 gave $p = 0.012$. However, application of the dissimilarity method with MRCA pairs from MRCALink gave significant p-values, evidence to reject the null hypothesis for both the full data and trimmed gopher-louse data sets.

With the full data sets and the trimmed data sets, applying **ParaFit** on all pairwise distances gave a significance at $p < 0.01$ for some sample fractions (Table 6). Applying **ParaFit** to the MRCALink-derived matrix for these full and trimmed data

sets also gave $p < 0.01$ for all sample fractions tried, indicating rejection of the null hypothesis.

DISCUSSION

Endophyte Codivergences with Hosts

In this study we have taken a novel approach to investigate codivergences between hosts and symbionts (parasites), which differs from others (Jackson, 2004; Legendre et al., 2002; Page and Charleston, 1998) in that it is a more direct comparison of historical cladogenesis events represented by inferred MRCA ages in ultrametric time trees in a way that avoids excessive weighting of deeper nodes compared with shallower nodes. The results indicate that, with relatively few exceptions, evolution of symbiotic epichloë fungi largely tracked evolution of their grass hosts. These symbioses extend across the taxonomic range of the Pooideae, including the basal tribe Brachyelytreae, yet are restricted to this subfamily. Endophytes related to epichloë (such as *Balansia* species) are known from other hosts, but the combination of very benign, often mutualistic, interactions and extremely efficient vertical transmission is known only in the Pooideae-epichloae system (Clay and Schardl, 2002). The conclusion that the system is dominated by codivergence implies that this unusually intimate symbiotic system emerged coincidentally with the emergence of this important grass subfamily.

In an earlier study comparing grass and endophyte evolutionary histories, the topological relationships of host tribes matched those of *Epichloë* species with a mixed mode of transmission (Schardl et al., 1997). However, no asexual lineages were included, and the possibility that some of the strictly sexual, horizontally transmitted species might also have a history of codivergence was not assessed. More importantly, the inference of codivergence was based on branching order, not relative timing of cladogenesis events. Although mirror phylogenies are suggestive of codivergence, it is the concomitance of corresponding cladogenesis events that defines codivergence

(Hafner et al., 1994). Conversely, unless the codivergences correspond to actual speciation events (that is, isolation of populations into distinct gene pools), lineage sorting effects, species duplications, and incomplete taxon sampling can prevent *H* and *P* phylogenies from mirroring each other (Page and Charleston, 1998). Therefore, we undertook the current study to assess codivergence by a more direct assessment of relative ages of corresponding cladogenesis events.

The null hypothesis was that relative ages of corresponding host and endophyte MRCAs were unrelated. If all sampled taxa were included, the null hypothesis was not rejected. This, however, was expected for the full data set for two reasons: (1) topology within the *E. typhina* clade bears no resemblance to that of the hosts, in keeping with the fact that *E. typhina* is a broad host-range species, and (2) some of the topological discordances in other clades strongly suggested occasional host jumps. Topological discordances tended to involve rarer associations. For example, *E. festucae* has only been identified in *K. cristata* once, but is very common in *Festuca* species. These features of the grass-endophyte system allowed for a rational basis for trimming trees of exceptions to assess support for codivergences in remaining taxa. When the *E. typhina* clade was removed the significance of codivergence increased dramatically. Using all pairwise distances for dissimilarity analysis the null hypothesis was still not rejected, but when the method was applied to the MRCALink-derived data set, the null hypothesis was strongly rejected. Trimming other possible host jumps further decreased the p-values in all analyses, strongly supporting the conclusion that the relationships between host and endophyte trees had a degree of dependence.

Various factors may cause a tendency for codivergence in evolution of these symbioses. For example, it may be much more likely for an endophyte to colonize a new host species that is closely related to its host of origin than a host that is more distantly related. A less likely (though not mutually exclusive) scenario would be speciation of hosts driven in part by adaptation to different symbionts. For example, considering that

benefits of these endophytes are likely to be highly dependent on environmental conditions, geographical separation of the combined host-endophyte systems followed by different selective forces in the separate populations might eventually lead to a circumstance (after the populations merge again) in which sharing of endophytes is less beneficial to the hosts. Analogously to the problem of hybrid disadvantage, a “hybrid symbiotum disadvantage” may simultaneously promote evolution of genetic isolation for both the hosts and their endophytes (Thompson, 1987).

However, it is also possible that hosts will tend to benefit from endophytes that have adapted to related hosts, but will benefit far less or actually suffer detriment from endophytes adapted to distantly related hosts. So, for example, most *E. typhina*, *E. baconii* and *E. glyceriae* strains infecting their hosts cause complete suppression of seed production, thus eliminating a means of dispersal (seeds) as well as a means of genetic diversification (meiotic recombination) that could enhance survivability of host progeny in the face of changing environmental factors. In contrast, endophytes such as *E. festucae*, *E. elymi*, *E. brachyelytri*, and *E. amarillans* allow substantial seed production by producing their fruiting structures (stromata) on only a portion of the tillers of the infected plant (Leuchtmann and Schardl, 1998; Schardl and Moon, 2003). The situation with *E. bromicola* and *E. sylvatica* is more complicated because expression of host seeds or endophyte stromata depends on host and endophyte genotypes, but these species also have the potential to be far less damaging to their hosts than are *E. typhina*, *E. baconii* and *E. glyceriae*. It should be much more to the benefit of a host to maintain compatibility with the benign or mutualistic *Epichloë* species than with the more antagonistic species. Indeed, *E. typhina* has a broad host range and clearly has not codiverged with those hosts (Leuchtmann and Schardl, 1998), which is why this species and the asexual endophytes most closely related to it were removed in the trimmed data sets for analysis of codivergence. The question is whether the remaining narrower host-range endophytes have tended to codiverge with their hosts, and our results suggest

that this is the case.

The possibility that these symbiotic systems emerged with the origin of the grass subfamily is intriguing. Kellogg (2001) postulated an early shift from shady to sunny habitats in subfamily Pooideae. According to this hypothesis, lineages derived following the split from the Brachyelytreae lineage moved into open habitats where, presumably, competition was less intense but solar radiation and drought were more prevalent. Additionally, such early colonizers may have been more conspicuous to potential herbivores. Protection from herbivory and drought are among the better documented effects of the epichloae (Clay and Schardl, 2002). Kellogg's hypothesis adds perspective to our results suggesting that codivergence between cool-season grasses and their endophytes originated with the Pooideae. It is reasonable to suggest that these symbioses may have played an important role in this habitat shift and that the mutualistic tendencies that these fungi commonly impart to their hosts (drought tolerance, herbivore resistance, etc.) are a direct reflection of these new selective pressures faced in open habitats. Even the more antagonistic endophytes that severely restrict seed production would probably have exerted a strong effect on structuring emerging grassland communities. Following this habitat transition, these symbionts may have significantly enhanced host fitness, aiding the radiation of a highly successful and speciose grass subfamily.

The MRCA Link Method

Our method involves direct comparison of MRCA ages rather than analysis of host and symbiont pairwise distance matrices, which is often used in studies of codivergence (Legendre et al., 2002). The pairwise distance approach is attractive in that it seems not to require inference of phylogenies, for which lineage sorting of preexisting polymorphisms, and imperfect genetic barriers between species, may give phylogenies that inaccurately represent histories of speciation (Page and Charleston, 1998). Nevertheless, there is a true phylogeny of species, and each pair of leaves (extant

taxa) for which a pairwise distance is calculated represents the node in that phylogeny that is their MRCA. Codivergence implies that the MRCA of a host leaf pair occurred at the same time as the MRCA of a symbiont leaf pair. If we test all host leaf pairs and corresponding symbiont leaf pairs in order to derive a statistical test of the null hypothesis that there is no significant relationship between host and symbiont MRCA times, a problem emerges in the number of times each MRCA is sampled. In the case of symmetrical and mirror (balanced) H and P trees, the frequency of node sampling ($= 2^{2m-2}$ where m is the level in the tree) increases exponentially as one goes deeper into the tree. For example, suppose we have the situation that both trees are balanced and the tree topologies are congruent. Then the MRCA pair constituting the roots of both trees is sampled $(n/2)^2$ times (where n is the number of taxa in each tree), whereas the MRCA pairs from corresponding tip clades are sampled only once. In this case, the number of times a MRCA pair is sampled is $(n_1 - 1)^2 + (n_2 - 1)^2$ where n_1 and n_2 are the numbers of descendants from the MRCAs in H and P trees, respectively. To examine the more generalized case of H and P trees that may not be balanced or congruent, 10,000 random H and P trees were generated with 25 taxa in PAML by the BDP with birth rates = 0.5, death rates = 0.5 and mutation rates = 100. Then, for each pair of H and P trees we identified all corresponding leaf pairs and counted how many times each MRCA pair was identified. The maximum number of times any MRCA pair was sampled averaged 111 in the 10,000 simulations.

In this study we introduce the MRCALink algorithm to specifically identify valid H and P MRCA pairs to compare divergence times, and to avoid repeated sampling of any MRCA pairs. The aforementioned analysis suggests that this method of sampling nodes is a substantial improvement over the use of complete pairwise distance matrices. However, the MRCA method is affected by incongruence of H and P trees. As shown in Figure 1, the nodes (MRCAs) of subtrees where such incongruences exist will tend to be sampled more than the nodes in congruent subtrees, even though each node pair is

sampled no more than once. This may be why, compared to the use of all pairwise distances, application of MRCALink is more sensitive to dependence between the trees being compared by the dissimilarity method in which the ML tree pair is compared to pairs of randomly generated trees of equal length. This may be considered a benefit of the MRCALink method, but further research into this behavior and possible modifications of the method are required to fully assess how this characteristic of the method affects inference about tree dependence.

Our method described in this paper does not find the minimum set of non-codiverging taxon pairs. It would be interesting to find an efficient algorithm to find the minimum set of non-codiverging taxon pairs from H and P .

Dissimilarity Method

The p-values obtained via the dissimilarity method for all pairwise distances tend to be larger than the p-values for MRCA pairs. This is because (1) analysis of all pairwise distances will generate a bias in favor of non-codivergence, (2) the S distribution is the sum of absolute values of differences between distances for each pair of taxa, and (3) from the Computation Results in the Analyses of Codivergence subsection above, if we take all pairwise distances, then we observed that MRCA pairs tend to be more frequently sampled in highly correlated trees than in poorly correlated trees. Since MRCA pairs for highly correlated T_H and T_P seem to be more frequently sampled among all pairwise distances than MRCA pairs for less correlated trees, the S value for T_H and T_P for all pairwise distances is overestimated and thus an estimated p-value obtained via the dissimilarity method with all pairwise distances is likely to be higher than the actual p-value (see Tables 3 – 6).

Generating random trees by the BDP tends to produce trees with long interior branches. Yang and Rannala (1997) suggest that taking incomplete species sampling into account generates more realistic trees. Thus we used **evolver** to generate random ultrametric trees with specified sampling fractions. Aris-Brosou and Yang (2003)

suggest using a sampling fractions in $(0, 0.001)$. However, Aris-Brosou and Yang (2003) also note that the sampling fraction is known to affect the topology of random trees, thus may affect divergence time of nodes. Therefore, in this study we took four different sampling fractions 0.0005, 0.001, 0.5 and 1, though we consider the smallest sampling fraction to be the most biologically relevant (Aris-Brosou and Yang, 2003).

We have used random trees to estimate the measure between two trees. Currently we use the BDP with a specified sampling fraction. When we measure a dissimilarity between the host and parasite trees in the space of trees, we used a heuristic method because measuring the exact distance between two trees in the space of trees requires exponential time in terms of the number of taxa (Billera et al., 2001). However, Amenta et al. (2007) recently developed a method to approximate a distance between trees in the space of trees efficiently, which could be a reasonable alternative to our method.

ParaFit Method

From results in Table 5 it seems that some of the p-values obtained via **ParaFit** with MRCA results are higher than the p-values via **ParaFit** with all pairwise distances. This may be due to the use of PCA prior to **ParaFit**. In the process of removing some of the entries in each distance matrix, we cut off more small signals in the data. However, we note that p-values for sub-optimal trees via **ParaFit** differ from p-values for the ML tree and in some instances have much larger p-value than p-values from the ML trees (e.g., Table 5). Also there are large differences between p-values from the ML trees and sub-optimal trees for the plant-endophyte data sets. For the ML trees **ParaFit** returns p-values of 0.001 for all data sets. However, with some of the sub-optimal trees **ParaFit** returns higher p-values not rejecting the null hypotheses. These sub-optimal trees are sampled from the distribution with the given data and model via MCMC.

Comparing the dissimilarity method and ParaFit method, both estimate the p-values by sampling random trees or random matrices, respectively. **ParaFit** takes two

distance matrices, then estimates the p-value by the permutation test. The dissimilarity method estimates the p-value by sampling random ultrametric trees from the BDP with a given sampling fraction known to be biologically meaningful. Also **ParaFit** does not include constraints that these random matrices are distance matrices and coming from trees. On the other hand, the dissimilarity method includes constraints that these random samples are ultrametric trees. Therefore, these biologically constraints added in the dissimilarity method should result in more biologically meaningful p-values. Also, it is interesting that the p-values computed from sub-optimal trees with T_4 data set did not give strong evidence for rejecting the hypothesis, but the ML method did. This suggests that the ParaFit method may be very sensitive to parametric assumptions and/or be unstable.

ACKNOWLEDGMENTS

We thank Adrian Leuchtman (ETH Zürich, Switzerland) for providing biological materials, Walter Hollin (University of Kentucky) for technical support, Stephane Aris-Brosou for very useful conversation, and Mark Hafner for providing the gopher-louse data sets. Also we would like to thank Roderic Page, Francois-Joseph Lapointe, Michael Charleston, Jack Sullivan, and an anonymous referee for very useful comments to improve this paper. This work was supported by National Science Foundation grant DEB-9707427, National Institutes of Health grant KY-INBRE P20 RR16481, U.S.Department of Agriculture grant CSREES Grant 2005-34457-15712, and the Harry E. Wheeler Endowment to the University of Kentucky Department of Plant Pathology. This is publication 08-12-034 of the Kentucky Agricultural Experiment Station, published with approval of the director.

REFERENCES

- Amenta, N., M. Godwin, N. Postarnakevich, and K. St. John. 2007. Approximating geodesic tree distance. *Inf. Proc. Lett.* 103:61–65.
- Aris-Brosou, S. and Z. Yang. 2002. Effects of models of rate evolution on estimation of divergence dates with special reference to the metazoan 18S ribosomal RNA phylogeny. *Syst. Biol.* 51:703–714.
- Billera, L. J., S. P. Holmes, and K. Vogtmann. 2001. Geometry of the space of phylogenetic trees. *Adv. Appl. Math.* 27:733–767.
- Bonnet, E. and Y. Van de Peer. 2002. zt: a software tool for simple and partial Mantel tests. *J. Stat. Softw.* 7:issue 10.
- Blanken, R. L., L. C. Klotz, and A. G. Hinnebusch. 1982. Computer comparison of new and existing criteria for constructing evolutionary trees from sequence data. *J. Mol. Evol.* 19:9–19.
- Brem, D., and A. Leuchtman. 1999. High prevalence of horizontal transmission of the fungal endophyte *Epichloë sylvatica*. *Bull. Geobotanical Inst. ETH* 65:3–12.
- Bull, J. J., I. J. Molineux, and W. R. Rice. 1991. Selection of benevolence in host-parasite system. *Evolution* 45:875–882.
- Catalán, P., P. Torrecilla, J. A. L. Rodriguez, and R. G. Olmstead. 2004. Phylogeny of the festucoid grasses of subtribe Loliinae and allies (Poeae, Pooideae) inferred from ITS and *trnL-F* sequences. *Mol. Phylogenet. Evol.* 31:517–541.
- Chung, K.-R., and C. L. Schardl. 1997. Sexual cycle and horizontal transmission of the grass symbiont, *Epichloë typhina*. *Mycol. Res.* 101:295–301.

- Clay, K., and J. Holah. 1999. Fungal endophyte symbiosis and plant diversity in successional fields. *Science* 285:1742-1744.
- Clay, K., and C. Schardl. 2002. Evolutionary origins and ecological consequences of endophyte symbiosis with grasses. *Amer. Nat.* 160:S99–S127.
- Craven, K. D., P. T. W. Hsiau, A. Leuchtmann, W. Hollin, and C. L. Schardl. 2001. Multigene phylogeny of *Epichloë* species, fungal symbionts of grasses. *Ann. Missouri Bot. Gard.* 88:14–34.
- Doyle, J. J., and L. L. Doyle. 1990. Isolation of plant DNA from fresh tissue. *Focus* 12:13–15.
- Drummond, A. J., and A. Rambaut. 2007. BEAST: Bayesian evolutionary analysis by sampling trees. *BMC Evol. Biol.* 7:214.
- Felsenstein, J. 1981. Evolutionary trees from DNA sequences: a maximum likelihood approach. *J. Mol. Evol.* 17:368–376.
- Freeman, E. M. 1904. The seed fungus of *Lolium temulentum* L., the darnel. *Phil. Trans. R. Soc. B* 196:1–27.
- Gentile, A., M. S. Rossi, D. Cabral, K. D. Craven, and C. L. Schardl. 2005. Origin, divergence, and phylogeny of epichloë endophytes of native Argentine grasses. *Mol. Phylogenet. Evol.* 35:196–208.
- Hafner, M. S., and S. A. Nadler. 1990. Cospeciation in host parasite assemblages: comparative analysis of rates of evolution and timing of cospeciation events. *Syst. Zool.* 39:192-204.
- Hafner, M. S., P. D. Sudman, F. X. Villablanca, T. A. Spradling, J. W. Demastes, and S. A. Nadler. 1994. Disparate rates of molecular evolution in cospeciating hosts and parasites. *Science* 265:1087-1090.

- Herre, E. A. 1993. Population structure and the evolution of virulence in nematode parasites of fig wasps. *Science* 259:1442-1445.
- Huelsenbeck, J. P., B. Rannala, and B. Larget. 2003. A statistical perspective for reconstructing the history of host-parasite associations. pp. 93-119 *in* Tangled trees: phylogeny, cospeciation, and coevolution (R. D. M. Page, ed.). University of Chicago Press, Chicago.
- Jackson, A. P. 2004. A reconciliation analysis of host switching in plant-fungal symbioses. *Evolution* 58:1909–1923.
- Kellogg, E. A. 2001. Evolutionary history of the grasses. *Plant Physiol.* 125:1198–1205.
- Legendre, P., Y. Desdevises, and E. Bazin. 2002. A statistical test for host–parasite coevolution. *Syst. Biol.* 51:217–234.
- Leuchtmann, A., and C. L. Schardl. 1998. Mating compatibility and phylogenetic relationships among two new species of *Epichloë* and other congeneric European species. *Mycol. Res.* 102:1169–1182.
- Moon, C. D., K. D. Craven, A. Leuchtmann, S. L. Clement, and C. L. Schardl. 2004. Prevalence of interspecific hybrids amongst asexual fungal endophytes of grasses. *Mol. Ecol.* 13:1455–1467.
- Moon, C. D., B. Scott, C. L. Schardl, and M. J. Christensen. 2000. The evolutionary origins of *Epichloë* endophytes from annual ryegrasses. *Mycologia* 92:1103–1118.
- Omacini, M., E. J. Chaneton, C. M. Ghersa, and C. B. Müller. 2001. Symbiotic fungal endophytes control insect host-parasite interaction webs. *Nature* 409:78-81.
- Page, R. D. M., and M. A. Charleston. 1998. Trees within trees: phylogeny and historical associations. *Trends Ecol. Evol.* 13:356–359.

- Piano, E., F. B. Bertoli, M. Romani, A. Tava, L. Riccioni, M. Valvassori, A. M. Carroni, and L. Pecetti. 2005. Specificity of host-endophyte association in tall fescue populations from Sardinia, Italy. *Crop Sci.* 45:1456–1463.
- Posada, D., and K. A. Crandall. 1998. Modeltest: testing the model of DNA substitution. *Bioinformatics* 14:817–818.
- Ronquist, F., and J. P. Huelsenbeck. 2003. MrBayes 3: bayesian phylogenetic inference under mixed models. *Bioinformatics* 19:1572–1574.
- Sampson, K. 1937. Further observations on the systemic infection of *Lolium*. *Trans. Brit. Mycol. Soc.* 21:84–97.
- Sampson, K. 1933. The systemic infection of grasses by *Epichloë typhina* (Pers.) Tul. *Trans. Brit. Mycol. Soc.* 18:30–47.
- Sanderson, M. J. 2002. Estimating absolute rates of molecular evolution and divergence times: A penalized likelihood approach. *Mol. Biol. Evol.* 19:101–109.
- Schardl, C. L., and A. Leuchtmann. 2005. The epichloë endophytes of grasses and the symbiotic continuum. Pages 475–503 *in* The Fungal community: its organization and role in the ecosystem (J. Dighton, J. F. White, and P. Oudemans, eds.). CRC Press, Boca Raton, Florida.
- Schardl, C. L., and C. D. Moon. 2003. Processes of species evolution in Epichloë/Neotyphodium endophytes of grasses. Pages 273–310 *in* Clavicipitalean fungi: evolutionary biology, chemistry, biocontrol and cultural impacts (J. F. White, Jr., C. W. Bacon, N. L. Hywel-Jones, and J. W. Spatafora, eds.). Marcel-Dekker, Inc., New York and Basel.
- Schardl, C. L., A. Leuchtmann, K.-R. Chung, D. Penny, and M. R. Siegel. 1997. Coevolution by common descent of fungal symbionts (*Epichloë* spp.) and grass hosts. *Mol. Biol. Evol.* 14:133–143.

- Soreng, R. J., and J. I. Davis. 1998. Phylogenetics and character evolution in the grass family (Poaceae): Simultaneous analysis of morphological and chloroplast DNA restriction site character sets. *Bot. Rev.* 64:1–85.
- Sullivan, T. J., and S. H. Faeth. 2004. Gene flow in the endophyte *Neotyphodium* and implications for coevolution with *Festuca arizonica*. *Mol. Ecol.* 13:649–656.
- Swofford, D. L. 1998. PAUP*: phylogenetic analysis using parsimony (*and other methods). Sinauer Associates, Sunderland, Massachusetts.
- Taberlet, P., L. Gielly, G. Pautou, and J. Bouvet. 1991. Universal primers for amplification of three non-coding regions of chloroplast DNA. *Plant Mol. Biol.* 17:1105–1109.
- Thompson, J. N. 1987. Symbiont-induced speciation. *Biol. J. Linn. Soc.* 32:385–393.
- Tredway, L. P., J. F. White, Jr., B. S. Gaut, P. V. Reddy, M. D. Richardson, and B. B. Clarke. 1999. Phylogenetic relationships within and between *Epichloë* and *Neotyphodium* endophytes as estimated by AFLP markers and rDNA sequences. *Mycol. Res.* 103:1593–1603.
- Tsai, H. F., J. S. Liu, C. Staben, M. J. Christensen, G. Latch, M. R. Siegel, and C. L. Schardl. 1994. Evolutionary diversification of fungal endophytes of tall fescue grass by hybridization with *Epichloë* species. *Proc. Natl. Acad. Sci. USA* 91:2542–2546.
- Yang, Z. 1997. PAML: a program package for phylogenetic analysis by maximum likelihood. *CABIOS* 15:555–556.
- Yang, Z. and B. Rannala. 1997. Bayesian phylogenetic inference using DNA sequences: a Markov chain Monte Carlo Method. *Mol. Biol. Evol.* 14:717–724.

APPENDIX

THE MRCA LINK ALGORITHM

Given a set of host taxa H and a set of symbiont taxa P (“parasites,” in keeping with other literature in the field), there is a map called $L : H \rightarrow P$ such that a host $A \in H$ has a parasite or symbiont $L(A) \in P$. Define $MRC A(A, B)$ to be the node representing the Most Recent Common Ancestor (MRCA) of leaves A and B .

Algorithm 1 (The MRCA Link Algorithm)

- **Input** *a set of host taxa H , a set of parasite taxa P , a H tree T_H , and a P tree T_P where n_1 is the number of taxa in H and n_2 is the number of taxa in P .*
- **Output** *a set of MRCA pairs of host taxa and parasite taxa.*
- **Algorithm**

Assign each node a unique number from 1 to $2n_1 - 1$ in the host tree and a unique number from 1 to $2n_2 - 1$ in the parasite tree such that a node i is ancestral to a node j .

Let U be a set of pairs of a pair of taxa in H and a pair of taxa in P , initially empty.

for (i from $n_1 + 1$ to $2n_1 - 1$) **do**{

Set $X_i = l_i \times r_i$ where l_i is the set of all left-descendants of i ,

and where r_i is the set of all right-descendants of i .

/ This is just another way of saying X_i is all such pairs of one leaf*

*from the left and one from the right. */*

while ($X_i \neq \emptyset$) **do**{

Choose $x = MRC A(a, b) \in X_i$ and identify $y_j = MRC A(L(a), L(b))$ for each distinct $L(a)$ and $L(b)$.

Remove x from X_i .

```

for (each distinct  $y_j$ ) do{
    if ( $MRC A(x, y_j) \notin U$ ) do{
         $U \leftarrow U \cup MRC A(x, y_j)$ .
    }
}
}
}
Output  $U$ .

```

Table 1. Hosts and symbionts. All listed taxa, as well as trimmed taxon sets T_1 – T_4 , were assessed for probability of codivergence.

Grasses	Endophytes	Included in:			
		T_1	T_2	T_3	T_4
<i>Brachyelytrum erectum</i> (root)	<i>Epichloë brachyelytri</i> (root)	+	+	+	+
<i>Brachypodium sylvaticum</i>	<i>Epichloë sylvatica</i> 200751	+	–	+	–
<i>Echinopogon ovatus</i>	<i>Neotyphodium aotearoae</i> 829	+	–	+	–
<i>Calamagrostis villosa</i>	<i>Epichloë baconii</i> 200745	+	+	+	+
<i>Agrostis tenuis</i>	<i>Epichloë baconii</i> 200746	+	+	+	+
<i>Agrostis hiemalis</i>	<i>Epichloë amarillans</i> 200744	+	+	+	+
<i>Sphenopholis obtusata</i>	<i>Epichloë amarillans</i> 200743	+	+	+	+
<i>Koeleria cristata</i>	<i>Epichloë festucae</i> 1157	+	+	–	–
<i>Lolium</i> sp. P4074	<i>Neotyphodium</i> sp. FaTG2 4074	+	+	+	+
<i>Lolium</i> sp. P4078	<i>Neotyphodium</i> sp. FaTG3 4078	+	+	+	+
<i>Lolium arundinaceum</i>	<i>Neotyphodium coenophialum</i> 19	+	+	+	+
<i>Lolium multiflorum</i>	<i>Neotyphodium occultans</i> 999	+	+	+	+
<i>Lolium edwardii</i>	<i>Neotyphodium typhinum</i> 989	–	–	–	–
<i>Lolium perenne</i>	<i>Epichloë typhina</i> 200736	–	–	–	–
<i>Lolium perenne</i>	<i>Neotyphodium lolii</i> 135	+	+	–	–
<i>Festuca rubra</i>	<i>Epichloë festucae</i> 90661	+	+	+	+
<i>Festuca longifolia</i>	<i>Epichloë festucae</i> 28	+	+	+	+
<i>Holcus mollis</i>	<i>Epichloë</i> sp. 9924	+	+	+	+
<i>Hordelymus europaeus</i>	<i>Neotyphodium</i> sp. 362	+	+	+	+
<i>Bromus ramosus</i>	<i>Epichloë bromicola</i> 201558	+	+	+	+
<i>Bromus erectus</i>	<i>Epichloë bromicola</i> 200749	+	+	+	+
<i>Bromus purgans</i>	<i>Epichloë elymi</i> 1081	+	+	–	–
<i>Hordeum brevisubulatum</i>	<i>Neotyphodium</i> sp. 3635	+	+	+	+
<i>Elymus canadensis</i>	<i>Epichloë elymi</i> 201551	+	+	+	+
<i>Glyceria striata</i>	<i>Epichloë glyceriae</i> 200755	+	+	+	+
<i>Achnatherum inebrians</i>	<i>Neotyphodium gansuense</i> 818	+	+	+	+

Table 2. Primer list. Oligonucleotide primers for amplification and sequencing of plant cpDNA intron and intergenic regions.

Primer	Region	Sequence (5'–3')	Orientation
B48557 ^a	trnT-trnLspacer	CATTACAAATGCGATGCTCT	downstream
A49291 ^a	trnT-trnLspacer	TCTACCGATTTTCGCCATATC	upstream
B49317 ^a	trnL intron	CGAAATCGGTAGACGCTACG	downstream
A49855 ^a	trnL intron	GGGGATAGAGGGACTTGAAC	upstream
B49873 ^a	trnL-trnF spacer	GGTTCAAGTCCCTCTATCCC	downstream
A50272 ^a	trnL-trnF spacer	ATTTGAACTGGTGACACGAG	upstream
trnTtrnL766-747u ^b	trnT-trnL spacer	GAATCATTGAATTCATCACT	upstream
trnTtrnL359-340u ^b	trnT-trnL spacer	TATTAGATTATTCGTCCGAG	upstream
trnTtrnL306-325d ^b	trnT-trnLspacer	GGAATTGGATTTTCAGATATT	downstream
trnTtrnL601-621d ^b	trnT-trnL spacer	AATATCAAGCGTTATAGTAT	downstream
P37.trnTtrnL.359-340u ^b	trnT-trnL spacer	TATTAGATTTCTCCTCTGAG	upstream
P56.trnTtrnL.378-398d ^b	trnT-trnL spacer	TAAGACGGGAGGTGGG	downstream
P56.trnTtrnL.398-378u ^b	trnT-trnL spacer	CTCCCCCACCTCCCGTCTTA	upstream
P57trnTtrnL556-576d ^b	trnT-trnL spacer	GTCATAGCAAATAAAATTGC	downstream
P2772.trnTtrnL.306-325d ^b	trnT-trnL spacer	CTAATTGGATTTTAGATATT	downstream
Bromus.trnTtrnL.177-197d ^b	trnT-trnL spacer	TTGATATGCTTAAGTATAGG	downstream
Bromus.trnTtrnL.197-177u ^b	trnT-trnL spacer	CCTATAGTTAAGCATATCAA	upstream
Bromus.trnTtrnL.357-376d ^b	trnT-trnL spacer	GCGTTATAGTATAATTTTG	downstream
Bromus.trnTtrnL.376-357u ^b	trnT-trnL spacer	CAAATTATACTATAACGC	upstream
trnLintron285-303d ^b	trnL intron	CATAGCAAACGATTAATCA	downstream
trnLintron303-285u ^b	trnL intron	TGATTAATCGTTTGCTATG	upstream
trnLtrnF.77-97d ^b	trnL-trnF spacer	TTTAAGATTCATTAGCTTTC	downstream

^a Primers used in PCR and sequencing.

^b Internal primers used in sequencing only.

Table 3. The p-values obtained by applying the dissimilarity method to all pairwise distances (noted by ALL) and to the MRCA Link-derived matrix (noted by MRCA) for full and $T_1 - T_4$ plant and endophyte data sets (see Table 1 for the data sets). SF means a sampling fraction.

Method	Data	SF = 0.0005	SF = 0.001	SF = 0.5	SF = 1.0
ALL	Full	0.784	0.783	0.677	0.374
MRCA	Full	0.123	0.123	0.081	0.039
ALL	T_1	0.117	0.115	0.035	0.009
MRCA	T_1	< 0.001	< 0.001	< 0.001	< 0.001
ALL	T_2	0.093	0.085	0.027	0.012
MRCA	T_2	< 0.001	< 0.001	< 0.001	< 0.001
ALL	T_3	0.064	0.061	0.017	0.005
MRCA	T_3	< 0.001	< 0.001	< 0.001	< 0.001
ALL	T_4	0.018	0.020	0.005	0.002
MRCA	T_4	< 0.001	< 0.001	< 0.001	< 0.001

Table 4. The p-values obtained using the dissimilarity method with sub-optimal trees with 26 full and $T_1 - T_4$ plant and endophyte data sets (all taxa listed in Table 1) via the Bayesian MCMC method in BEAST. ALL means the dissimilarity method with all pairwise distances, and MRCA means the dissimilarity method with the MRCALink-derived matrix. SF means a sampling fraction. Each sampled tree is assigned a number from 1 to 3 to distinguish it from the others.

Method	Data	sample number	SF = 0.0005	SF = 0.001	SF = 0.5	SF = 1.0
ALL	Full	sample 1	0.700	0.686	0.466	0.294
MRCA	Full	sample 1	0.011	0.011	0.003	0.002
ALL	Full	sample 2	0.474	0.483	0.245	0.119
MRCA	Full	sample 2	0.064	0.064	0.025	0.014
ALL	Full	sample 3	0.684	0.683	0.450	0.262
MRCA	Full	sample 3	0.193	0.190	0.102	0.061
ALL	T_1	sample 1	0.451	0.448	0.236	0.115
MRCA	T_1	sample 1	< 0.001	< 0.001	< 0.001	< 0.001
ALL	T_1	sample 2	0.029	0.033	0.005	< 0.001
MRCA	T_1	sample 2	< 0.001	< 0.001	< 0.001	< 0.001
ALL	T_1	sample 3	0.006	0.007	< 0.001	< 0.001
MRCA	T_1	sample 3	< 0.001	< 0.001	< 0.001	< 0.001
ALL	T_2	sample 1	0.346	0.355	0.190	0.097
MRCA	T_2	sample 1	< 0.001	< 0.001	< 0.001	< 0.001
ALL	T_2	sample 2	0.355	0.360	0.184	0.099
MRCA	T_2	sample 2	< 0.001	< 0.001	< 0.001	< 0.001
ALL	T_2	sample 3	0.084	0.079	0.022	0.010
MRCA	T_2	sample 3	< 0.001	< 0.001	< 0.001	< 0.001
ALL	T_3	sample 1	0.070	0.067	0.020	0.007
MRCA	T_3	sample 1	< 0.001	< 0.001	< 0.001	< 0.001
ALL	T_3	sample 2	0.030	0.029	0.007	0.030
MRCA	T_3	sample 2	< 0.001	< 0.001	< 0.001	< 0.001
ALL	T_3	sample 3	0.132	0.138	0.050	0.021
MRCA	T_3	sample 3	< 0.001	< 0.001	< 0.001	< 0.001
ALL	T_4	sample 1	0.106	0.103	0.039	0.015
MRCA	T_4	sample 1	< 0.001	< 0.001	< 0.001	< 0.001
ALL	T_4	sample 2	0.024	0.026	0.007	0.002
MRCA	T_4	sample 2	< 0.001	< 0.001	< 0.001	< 0.001
ALL	T_4	sample 3	0.017	0.016	0.006	0.002
MRCA	T_4	sample 3	< 0.001	< 0.001	< 0.001	< 0.001

Table 5. The p-values obtained through ParaFit to all pairwise distances (ALL) and to the MRCAlink-derived matrix (MRCA) for the sub-optimal trees of 26 full and $T_1 - T_4$ plant and endophyte data sets. The sub-optimal trees were chosen as samples of the most common likelihood trees. This was done by choosing samples with tree likelihoods close to the mean of all 10,000 tree likelihoods. For each data set, the three sampled sub-optimal trees were arbitrarily assigned a number from 1 to 3.

Method	Data	Sample 1	Sample 2	Sample 3
ALL	Full	0.146	0.007	< 0.001
MRCA	Full	0.097	0.014	0.020
ALL	T_1	0.011	0.003	0.006
MRCA	T_1	0.023	0.029	0.115
ALL	T_2	< 0.001	< 0.001	0.004
MRCA	T_2	< 0.001	0.033	0.033
ALL	T_3	0.003	< 0.001	0.002
MRCA	T_3	0.015	< 0.001	0.017
ALL	T_4	0.046	0.046	0.042
MRCA	T_4	0.108	0.084	0.066

Table 6. The p-values obtained using the dissimilarity method for the gopher and louse data. The full data set includes all hosts and parasites from (Hafner et al., 1994), whereas for the trimmed data set data were removed for the gophers and lice which are from (Huelsenbeck et al., 2003). ALL means the dissimilarity method with all pairwise distances and MRCA means the dissimilarity method with the MRCA Link-derived matrix.

Method	Data	SF = 0.0005	SF = 0.001	SF = 0.5	SF = 1.0
ALL	Full	0.589	0.577	0.394	0.248
MRCA	Full	0.002	0.003	< 0.001	< 0.001
ALL	Trimmed	0.012	0.015	0.006	0.003
MRCA	Trimmed	< 0.001	< 0.001	< 0.001	< 0.001

Legends to Figures

Figure 1. Simple examples of congruent and incongruent H and P trees, where H is a set of plant or animal hosts and P is a set of their symbionts or parasites, demonstrating the relationships of MRCA (most recent common ancestor) pairs to their corresponding H and P taxon pairs. In an ultrametric time tree, the distance between any two taxa is twice the age of their MRCA. In each tip clade a MRCA uniquely relates two taxa, but a MRCA deeper in the tree relates multiple taxon pairs. Therefore, pairwise distance matrices represent tip clade MRCAs once, but deeper MRCAs multiple times. The effect on sampling MRCA pairs is illustrated below each tree. For both congruent and incongruent pairs of H and P trees, comparison of pairwise distance matrices gives greater representation to pairs that include deeper MRCAs than to pairs of shallower MRCAs. The MRCALink algorithm samples corresponding H and P MRCA pairs only once.

Figure 2. Majority rule consensus tree with average branch lengths from Bayesian with General Time-Reversible plus gamma distribution (GTR+G) analysis of cpDNA intron and intergenic sequences from pooid grasses. The first number in each pair is a posterior probability and the second number in each pair indicates bootstrap support percentages (if > 50%) obtained by 1000 maximum parsimony searches with branch swapping. Currently accepted tribes are indicated at right. Full taxon names are given in Table 1.

Figure 3. Majority rule consensus tree with average branch lengths from Bayesian (GTR+G) analysis from mainly intron sequences of endophyte *tefA* and *tubB* genes. Branches are labeled with posterior probability followed by bootstrap support percentage (if over 50%) obtained by 1000 maximum parsimony searches with branch swapping. Host species are indicated in parentheses. Full taxon names are given in Table 1. The LAE (*Lolium*-associated endophyte) clade is labeled.

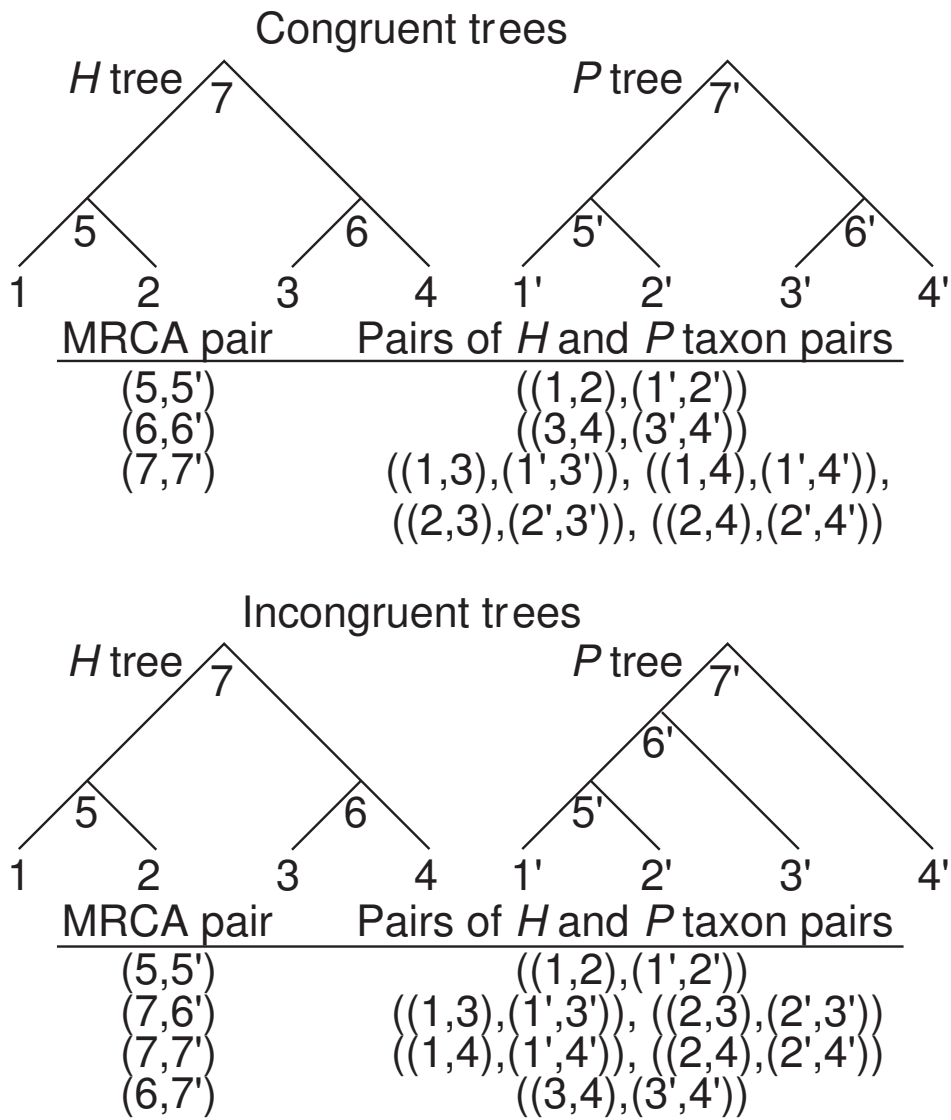
Figure 4. Ultrametric maximum likelihood (ML) time trees for host grasses and their endophytes. Hosts and their endophytes are indicated by dashed lines. Full taxon names are

given in Table 1. Numeric values on nodes represent their posterior probabilities estimated by BEAST. The individual node posterior probabilities were calculated from nodes with a posterior probability greater than 0.5, by **Tree Annotator** in the BEAST package. Labels preceding endophyte names indicate *H* and *P* pairs retained in trimmed data sets T_1 – T_4 . The LAE (*Lolium*-associated endophyte) clade is labeled.

Figure 5. Plots of relative MRCA ages of hosts (H) and their corresponding endophytes (P) identified by the MRCALink algorithm from ultrametric ML trees for the full dataset or trimmed datasets T_1 – T_4 , as indicated (see Table 1).

Figure 6. Ultrametric ML time trees for gopher and louse data sets (Hafner et al., 1994) constructed via BEAST. Hosts and their parasites are indicated by connecting dashed lines. Genera: *O.* = *Orthogeomys*, *Z.* = *Zygogeomys*, *P.* = *Pappogeomys*, *C.* = *Cratogeomys*, *G.* = *Geomys*, *T.* = *Thomomys*, *Gd.* = *Geomydoecus*, *Td* = *Thomomydoecus*.

Figure 1.

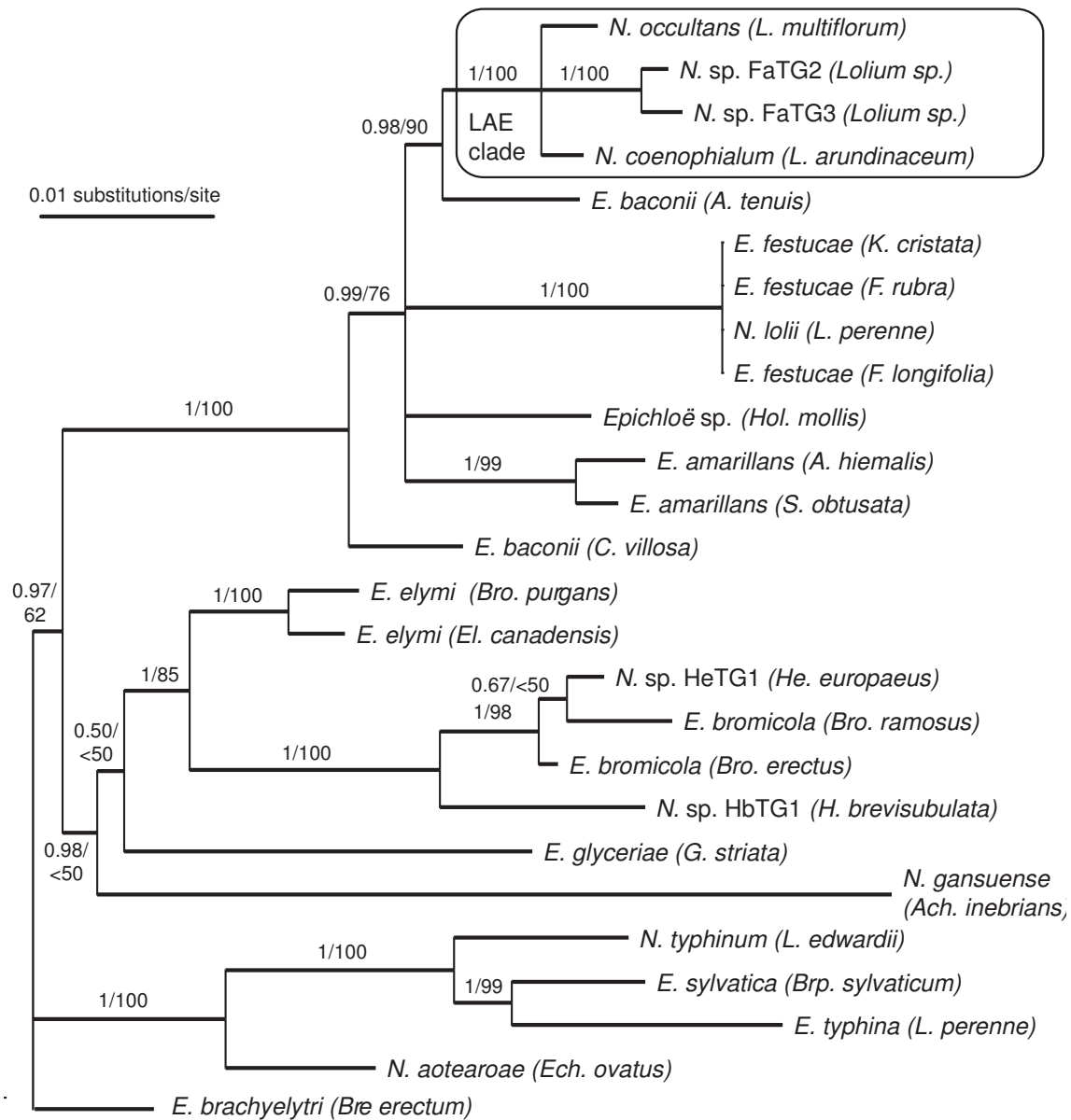


0.01 substitutions/site

A. tenuis
A. hiemalis
C. villosa
Ech. ovatus
K. cristata
S. obtusata
L. edwardii
L. multiflorum
L. perenne
L. arundinaceum
Lolium sp. P4074
Lolium sp. P4078
F. rubra
F. longifolia
Hol. mollis
Bro. erectus
Bro. purgans
Bro. ramosus
He. europaeus
El. canadensis
H. brevisubulatum
Brp. sylvaticum
Ach. inebrians
G. striata
Bre. erectum

Agrostideae
Poeae
Bromeae
Hordeae
Brachypodieae
Stipeae
Meliceae
Brachyelytreae

Figure 3.



Phylogenetic trees for three gene regions: T1, T2, and T3. The T1 tree (left) shows relationships between various grass species, with a scale bar of 0.01 substitutions/site. The T2 tree (middle) shows relationships between the same species, with a scale bar of 0.01 substitutions/site. The T3 tree (right) shows relationships between the same species, with a scale bar of 0.01 substitutions/site. The T1 and T2 trees are rooted at the bottom, while the T3 tree is rooted at the top. The T1 and T2 trees show a clear separation between the T1 and T2 clades, while the T3 tree shows a more complex relationship between the T1 and T2 clades.

Species and their corresponding gene regions (T1, T2, T3) are listed in the center of the figure:

- Br. erectum* ----- T1,2,3,4
- Ach. inebrians* ----- T1,2,3,4
- G. striata* ----- T1,2,3,4
- El. canadensis* ----- T1,2,3,4
- H. brevisubulatum* ----- T1,2
- He. eurupaeus* ----- T1,2,3,4
- Bro. ramosus* ----- T1,2,3,4
- Bro. erectus* ----- T1,2,3,4
- Bro. purgans* ----- T1,2
- Lolium* sp. P4078 ----- T1,2,3,4
- Lolium* sp. P4074 ----- T1,2,3,4
- L. arundinaceum* ----- T1,2,3,4
- L. multiflorum* ----- T1,2,3,4
- L. edwardii* ----- T1,2,3,4
- L. perenne* ----- T1,2
- F. rubra* ----- T1,2,3,4
- F. longifolia* ----- T1,2,3,4
- Hol. mollis* ----- T1,2
- A. tenuis* ----- T1,2,3,4
- A. hiemalis* ----- T1,2,3,4
- C. villosa* ----- T1,2,3,4
- Ech. ovatus* ----- T1,3
- K. cristata* ----- T1,3
- S. obtusata* ----- T1,3
- Brp. sylvaticum* ----- T1,3
- E. brachyelytri* ----- T1,2,3,4
- N. gansuense* ----- T1,2,3,4
- E. glyceriae* ----- T1,2,3,4
- E. elymi* ----- T1,2,3,4
- N. sp. HbTG1* ----- T1,2,3,4
- N. sp. HeTG1* ----- T1,2,3,4
- E. bromicola* ----- T1,2,3,4
- N. sp. FaTG2* ----- T1,2,3,4
- N. sp. FaTG3* ----- T1,2,3,4
- N. coenophialum* ----- T1,2,3,4
- N. occultans* ----- T1,2,3,4
- E. baconii* ----- T1,2,3,4
- N. lolli* ----- T1,2,3,4
- E. festucae* ----- T1,2,3,4
- E. festucae* ----- T1,2,3,4
- Epichloë* sp. ----- T1,2,3,4
- E. amarillans* ----- T1,2,3,4
- E. amarillans* ----- T1,2,3,4
- E. baconii* ----- T1,2,3,4
- N. aotearoae* ----- T1,2,3,4
- N. typhinum* ----- T1,2,3,4
- E. typhina* ----- T1,2,3,4
- E. sylvatica* ----- T1,2,3,4

Figure 5.

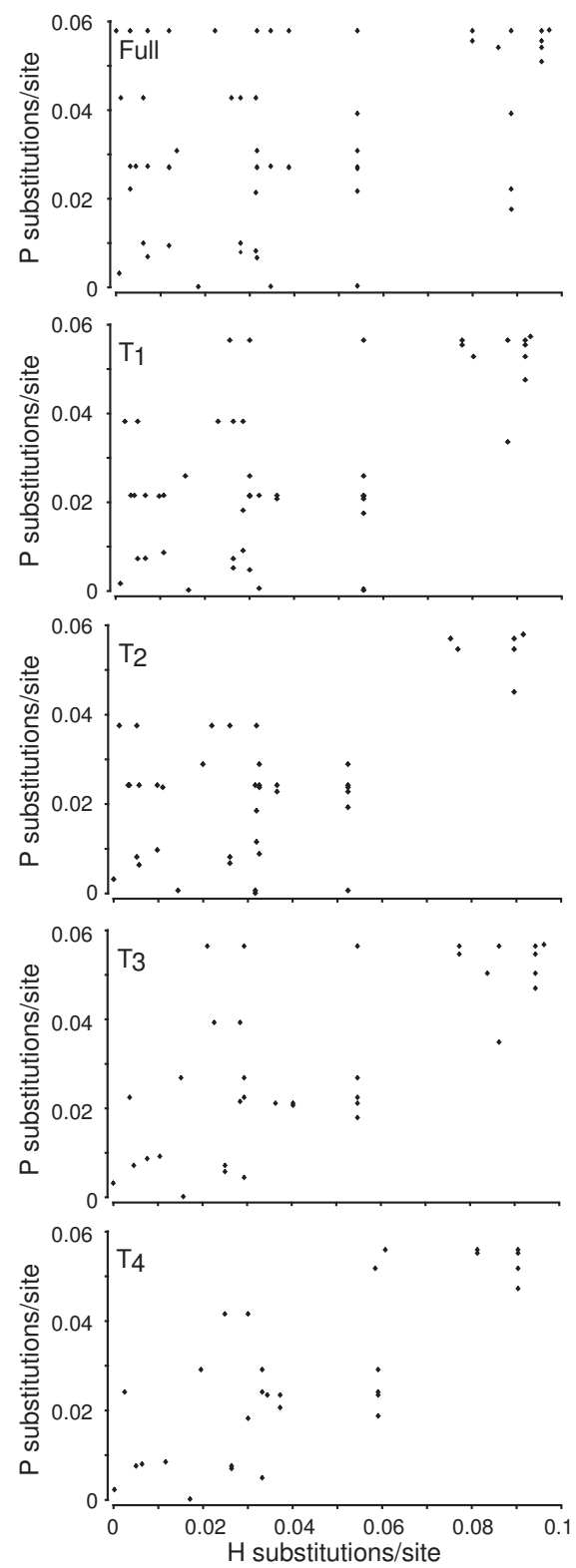


Figure 6.

